fire

Article

Fuel Resistance of Firefighting Surfactant Foam Formulations

Ayşenur Ateş *, Rui Qiao and Brian Y. Lattimer *

Department of Mechanical Engineering, Virginia Tech, Blacksburg, VA 24061, USA; ruiqiao@vt.edu
* Correspondence: aysenur@vt.edu (A.A.); lattimer@vt.edu (B.Y.L.)

Abstract: Aqueous film-forming foam (AFFF) is widely recognized for its excellent fire-extinguishing capabilities, yet the specific roles of its components remain insufficiently understood. AFFF typically consists of fluorocarbon and hydrocarbon surfactants, as well as organic solvents such as diethylene glycol butyl ether (DGBE), which can significantly influence foam performance. This study investigates the effects of surfactant mixtures and the DGBE additive on foam stability and fuel resistance at room temperature and ambient humidity. Static foam ignition experiments were conducted to assess fuel transport through foams using various hydrocarbon fuels, including n-octane, iso-octane, n-heptane, methylcyclohexane, methylcyclopentane, and a mixture of 25% trimethylbenzene with 75% n-heptane. Methylcyclopentane, with its higher vapor pressure and solubility, led to the shortest ignition times, indicating faster fuel transport. The addition of DGBE increased ignition times by a factor of 1.2 to 3.7 for individual surfactants, while the Capstone+Glucopon mixture improved ignition times by a factor of 2.4 to 5.5 compared to the individual surfactants. Further enhancement was observed with Capstone+Glucopon+DGBE, increasing ignition times by a factor of 3 to 7.3 compared to the individual surfactants. Additionally, combining DGBE with surfactant mixtures reduced fuel concentration in the bulk solution by over 60% compared to individual surfactants, significantly enhancing fuel resistance. Interface experiments showed that fuel presence, particularly methylcyclopentane and n-octane, altered the foam structure and accelerated drainage at the foam/fuel interface, impacting foam stability and fuel transport. These findings demonstrate that surfactant mixtures and DGBE-enhanced formulations substantially improve foam stability and fuel resistance.

Keywords: surfactant mixture effect; additive effect; foam stability; fuel resistance; foam/fuel interface

check for updates

Academic Editor: Kaihua Lu

Received: 10 December 2024
Revised: 12 January 2025
Accepted: 22 January 2025
Published: 25 January 2025

Citation: Ateş, A.; Qiao, R.; Lattimer, B.Y. Fuel Resistance of Firefighting Surfactant Foam Formulations. *Fire* **2025**, *8*, 44. https://doi.org/10.3390/fire8020044

Copyright: © 2025 by the authors. Licensee MDPI, Basel, Switzerland. This article is an open access article distributed under the terms and conditions of the Creative Commons Attribution (CC BY) license (https://creativecommons.org/licenses/by/4.0/).

1. Introduction

Surface-active agents (surfactants) are integral to firefighting foams and are widely studied due to their amphiphilic structures, which consist of a hydrophilic head and a hydrophobic tail [1–7]. These surfactants are commonly categorized based on the nature of their hydrophobic groups, including fluorocarbon (FC), hydrocarbon (HC), and silicone. Each class of surfactant contributes uniquely to the performance of firefighting foams, with fluorocarbon surfactants being particularly effective in suppressing fires involving liquid fuels due to their ability to significantly reduce surface tension and facilitate rapid formation of a protective aqueous film [8,9].

Aqueous film-forming foam (AFFF) has been extensively used for fire suppression due to its ability to rapidly extinguish pool fires [3,10–14]. It is typically composed of fluorocarbon surfactants (e.g., Capstone), hydrocarbon surfactants (e.g., Glucopon), an organic solvent such as diethylene glycol butyl ether (DGBE), and water. Despite its effectiveness, the environmental persistence and toxicity of fluorocarbon surfactants have led to increasing regulatory restrictions and bans [15–19]. While numerous studies have investigated the roles of individual surfactants in AFFF formulations [9,20], much of the existing research focuses on the overall fire suppression capabilities of AFFF [12,21]. These studies explore aspects such as film formation [10], rheology properties [22,23], foam drainage behavior [1,24,25], and burn back performance [8,26]. However, a fundamental understanding of the contributions of individual components to AFFF performance in firefighting applications remains limited, leaving significant gaps in the literature that warrant further investigation.

Fluorocarbon surfactants are highly effective in fire extinguishment due to their unique physicochemical properties [15,27]. However, their environmental persistence and toxicity have prompted the need for fluorine-free alternatives [1,9,21,28]. Compared to hydrocarbon surfactants, fluorocarbon surfactants exhibit notable differences in structure and behavior [29,30], which can significantly influence their performance and interactions within foam solutions. Their reduced dispersion interactions and larger perfluoroalkyl moieties promote self-assembly at the air–water interface, lowering surface energy and improving the spreading coefficient on hydrocarbon fuels [31]. The underlying mechanisms by which these differences influence foam performance require further investigation, particularly to guide the development of future fluorine-free surfactant formulations. Recent research has explored the use of fluorine-free surfactants, such as PEO–PPO–PEO triblock copolymers, to enhance foam stability under extreme conditions. These copolymers have demonstrated improved performance by forming thermo-responsive foam films that transition from mobile to rigid states at elevated temperatures, significantly improving foam stability during pool fire suppression [18]. Such advancements highlight the potential of fluorine-free surfactant formulations to achieve fire extinguishment performance comparable to that of AFFF.

Several studies have highlighted that mixtures of surfactants can improve fire extinguishment performance compared to individual surfactants [11,12]. For example, Sheng et al. [32] demonstrated that surfactant mixtures exhibit higher foaming ability due to enhanced molecular interactions between the components. Similarly, Giles et al. [33] investigated the fire suppression performance of a fluorocarbon surfactant with and without the addition of DGBE using heptane as a fuel. Similarly, the use of low-carbon alcohols as additives in hydrocarbon and silicone-based surfactant systems has been shown to block foam liquid channels, delay drainage, and increase foam stability, resulting in better cooling effects and overall fire suppression efficiency [19]. These findings suggest that tailored surfactant formulations, combined with appropriate additives, can enhance foam performance under challenging fire conditions. Despite these advancements, there still remains a need for further research to fully understand how the properties of surfactant mixtures and additives influence the fuel transport dynamics of firefighting foams. Additionally, exploring the underlying mechanisms at the interface is crucial for optimizing foam formulations for fire suppression applications.

Understanding foam stability is essential for developing advanced fluorine-free fire-extinguishing agents. The interfaces between foam/solution and foam/fuel are critical in understanding the mechanisms of fuel transport through surfactant-based systems. At the foam/solution interface, surfactants play a pivotal role in stabilizing foam structures by reducing surface tension, controlling bubble size, and regulating drainage rates. These factors directly influence the foam's ability to act as a physical and chemical barrier against fuel infiltration [34]. In contrast, the foam/fuel interface is defined by the interactions between surfactant molecules and fuel, which govern the rate at which fuel penetrates or spreads through the foam matrix. This interface is particularly significant because the presence of fuel can disrupt surfactant-stabilized films, compromising foam stability and altering foam dynamics. Such disruptions may lead to accelerated drainage, reduced bubble integrity, and diminished barrier performance [26,35,36]. Understanding these interfacial interactions is crucial for optimizing firefighting foam formulations to enhance fuel resistance and maintain stability under challenging conditions.

This study examines the foam behavior of Capstone and Glucopon surfactants, both individually and in mixtures (Capstone+Glucopon), with and without the addition of DGBE (Capstone+DGBE, Glucopon+DGBE, and Capstone+Glucopon+DGBE). A commercial AFFF formulation was also evaluated for comparison. These experiments aim to provide critical insights into the effects of surfactant mixtures and their interactions with DGBE, shedding light on fuel transport mechanisms within the foam matrix and through the aqueous solution. A dynamic foam analyzer (DFA) was employed to measure key foam characteristics, including mean bubble diameter, expansion ratio (ER), and 25% liquid drainage time, under conditions with and without hydrocarbon fuels (methylcyclopentane and n-octane). Furthermore, the interfacial properties at both the foam/solution and foam/fuel interfaces were analyzed to understand their influence on foam stability and fuel transport. Fuel concentrations in the aqueous surfactant solutions were also quantified. Additionally, ignition times were recorded for each fuel-surfactant combination, offering deeper insights into the fuel resistance of the foams and their capacity to mitigate fuel transport.

2. Materials

2.1. Surfactants

Seven different surfactant solutions were prepared to investigate the effect of mixing and additive on the mechanisms of fuel transport. Capstone 1157 (Chemours, Inc., Wilmington, DE, USA; purity $\geq$ 99%) is a fluorocarbon surfactant with a tail length of six carbons and a zwitterionic head group, containing 27% active surfactant. In contrast, Glucopon 600 CS UP (Sigma-Aldrich, Inc., St. Louis, MO, USA; purity $\geq$ 98%) is a hydrocarbon surfactant with a tail length of 12 carbons and a non-ionic head group, containing 50% active surfactant. Pure ($\geq$99%) diethylene glycol butyl ether (DGBE), supplied by Sigma-Aldrich, Inc., was used as the organic solvent. To explore the role of DGBE, surfactant concentrates of Capstone+DGBE and Glucopon+DGBE were created.

AFFF (6% concentrate, Chemguard, Inc., Marinette, WI, USA), a perfluoroalkyl substance containing both fluorocarbon and hydrocarbon surfactants along with DGBE, was included for comparison. Surfactant mixtures, including Capstone+Glucopon and Capstone+Glucopon+DGBE, were prepared using Capstone 1157, Glucopon 600 CS UP, and DGBE as the components.

2.2. Surfactant Mixtures and Concentrate Preparation

The main constituents of the mixture formulations were Capstone 1157 (Chemours, Inc., Wilmington, DE, USA), Glucopon 600 CS UP (Sigma-Aldrich, Inc., St. Louis, MO, USA), and diethylene glycol monobutyl ether (DGBE, Sigma-Aldrich, Inc., St. Louis, MO, USA), all used without further modifications. Due to differences in the active surfactant content between the surfactant concentrates, Capstone 1157 contains 27% active surfactant, while Glucopon contains 50% active surfactant, the amounts of surfactant concentrate added to the formulations were adjusted accordingly.

Based on the literature [9], the surfactant mixture concentrate with DGBE was prepared by precisely mixing 2.5 parts Glucopon, 3 parts Capstone, 5 parts DGBE, and 20 parts distilled water by mass. In contrast, the surfactant mixture without DGBE (Capstone+Glucopon) was prepared using the same proportions of Glucopon and Capstone but replacing the 5 parts of DGBE with additional distilled water, resulting in a total of 25 parts distilled water.

The Capstone+DGBE concentrate was created by mixing 7.54 parts of Capstone, 5 parts of DGBE, and 20 parts of distilled water by mass. Similarly, the Glucopon+DGBE concentrate was prepared by mixing 4.15 parts of Glucopon, 5 parts of DGBE, and 20 parts of distilled water. These individual surfactant+DGBE formulations were prepared to maintain the same active surfactant content as the surfactant mixtures (Capstone+Glucopon) with and without DGBE, ensuring consistency across the different formulations.

Finally, the individual surfactant concentrates (without DGBE) were prepared using only Capstone or Glucopon with distilled water at the appropriate ratios.

2.3. Fuels

The ignition experiments have been performed using five types of fuels, n-octane (Calpac Lab, Inc., Novato, CA, USA; purity ≥ 99%), iso-octane (Thermo Fisher Scientific, Inc., Waltham, MA, USA; purity ≥ 98%), n-heptane (Alfa Aesar, Inc., Waltham, MA, USA; purity ≥ 99%), methylcylohexane (Calpac Lab, Inc., Novato, CA, USA; purity ≥ 98%), and methylcyclopentane (MCP, Calpac Lab, Inc., Novato, CA, USA; purity ≥ 98%). On the other hand, ignition experiments with a fuel mixture were performed using 25% 1,2,4 trimethylbenzene (TMB, Sigma Aldrich, Inc., St. Louis, MO, USA; purity ≥ 99%) and 75% n-heptane. Table 1 presents detailed information on the properties of the fuels used in the experiments. This includes key parameters such as water solubility and vapor pressure, which are essential in understanding the behavior of the fuels during the foam application and firefighting process. Table 1 indicates that methylcyclohexane and methylcyclopentane have greater water solubility than other fuels, with the exception of 1,2,4-trimethylbenzene (TMB) and its mixture with n-heptane. This could potentially aid in the transport of fuel into the foam. Methylcyclopentane has the highest vapor pressure among the fuels, which could enhance fuel transport by causing fuel vapor to rise into the foam more than the other fuels.

Table 1. Fuel properties at 25 °C for fuels from Thermo Fisher Scientific SDS [37–42].

Fuel	Solubility at 25 °C (mg fuel L^{-1} Water)	Vapor Pressure at 25 °C	Flashpoint (°C)
n-Octane	0.66	14	13
Iso-Octane	0.66	45	−12
n-Heptane	3.4	46	−7
1,2,4-Trimethylbenzene	57	2	48
25% 1,2,4-Trimethylbenzene + 75% n-Heptane	15.75	35	-
Methylcyclohexane	14	49	−20
Methylcyclopentane	14	138	−37

These fuels were selected to explore the impact of key fuel properties, such as vapor pressure and water solubility, on fuel transport through foam. The selection includes a range of branched, cyclic, and linear hydrocarbons, enabling a systematic investigation of how specific properties influence foam performance. For instance, n-octane and iso-octane have the same water solubilities but differ in vapor pressures, while iso-octane, n-heptane and methylcyclohexane have similar vapor pressures but differ in water solubilities. Additionally, methylcyclohexane and methylcyclopentane have the same water solubilities but differ significantly in vapor pressures, allowing the effect of vapor pressure on fuel transport to be investigated. This approach provides insights into the role of individual fuel characteristics in foam stability and fuel resistance. Furthermore, the inclusion of a fuel mixture (25% trimethylbenzene + 75% n-heptane) simulates complex real-world firefighting scenarios, such as those involving gasoline, thereby offering a comprehensive understanding of foam behavior in diverse conditions.

3. Methods

3.1. Surface Tension Measurements

The Wilhelmy plate method [43] was used to measure the surface tension and critical micelle concentration (CMC) of surfactant solutions at 25 °C using a KRÜSS K100 tensiometer (KRÜSS Scientific, Matthews, NC, USA). Surface tension was recorded for surfactant solutions at varying concentrations, decreasing until the CMC was reached, beyond which further reduction was prevented by micelle formation. The surface tension and CMC results of used surfactants are presented in Table 2. Additionally, surface tension measurements and interfacial tension measurements with water for all fuels were also performed using the same instrument, and the results are presented in Figure 1a and Figure 1b, respectively.

Table 2. The surface tension [mN/m] and CMC values of the surfactants at 25 °C.

Surfactant	γ_{CMC} [mN/m]	CMC
Capstone	16.0	0.0110 [wt.%]
Glucopon	28.5	0.0120 [wt.%]
Capstone+DGBE	15.8	0.0090 [wt.%]
Glucopon+DGBE	28.1	0.0037 [wt.%]
Capstone+Glucopon	17.4	0.0096 [wt.%]
Capstone+Glucopon+DGBE	17.1	0.0420 [wt.%]
6% AFFF	17.4	0.4500 [vol.%]

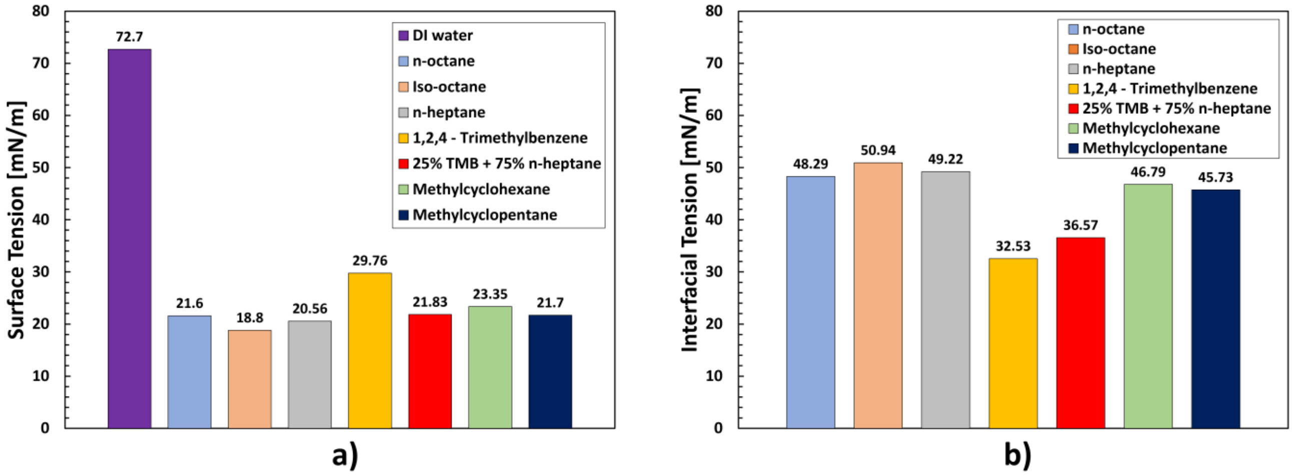

Figure 1. (**a**) Surface tension of fuels and (**b**) Interfacial tension of fuels with water at 25 °C.

All the experiments were conducted at 5X CMC, consistent with the concentration used in the reference [9].

3.2. Foam Generation and Characterization

A dynamic foam analyzer (DFA100, KRÜSS Scientific, Matthews, NC, USA) was used to investigate foam expansion ratio, 25% liquid drainage time [s], and mean bubble diameter [µm] with time. For this purpose, 35 mL of aqueous solution was poured into a glass cylinder with a 40 mm diameter. Once the aqueous liquid solution has been poured into the glass cylinder, it is important to ensure that no foam has formed. A sparger with 16 to 40 µm porosity provides airflow for 40 s and forms foam bubbles. The real image of the DFA setup is given in Figure 2. As soon as foam generation occurred, the expansion ratio was calculated. The expansion ratio is calculated as:

$$ER = \frac{V_{foam}}{V_{initial,liquid} - V_{final,liquid}} \tag{1}$$

where V_{foam} is the foam volume at 40 s (airflow stops), $V_{initial,liquid}$ is the initial liquid volume corresponding to 35 mL, and $V_{final,liquid}$ is the final liquid volume after airflow stops. Therefore, the expansion ratio (ER) for each surfactant solution was determined using foam and aqueous liquid volumes recorded in real time by Lab-View. This setup allowed continuous monitoring of foam formation and drainage throughout the duration of the experiment. A camera with a 1670 × 1 pixel resolution, positioned in line with a laser, was used to capture high-resolution images of foam bubbles at desired time intervals (ranging from 0 s to 5000 s). These images were essential for tracking the evolution of foam structure and bubble size over time. The captured images were processed using ADVANCE software (version 1.15), which provided detailed analysis of foam parameters, including foam and liquid volumes (in mL) and the 25% liquid drainage time (in seconds). The 25% liquid drainage time corresponds to the time required for 25% of the initial liquid volume to drain from the foam, a critical metric for evaluating foam stability. By combining real-time monitoring with image-based analysis, this approach ensured accurate and reliable quantification of foam properties.

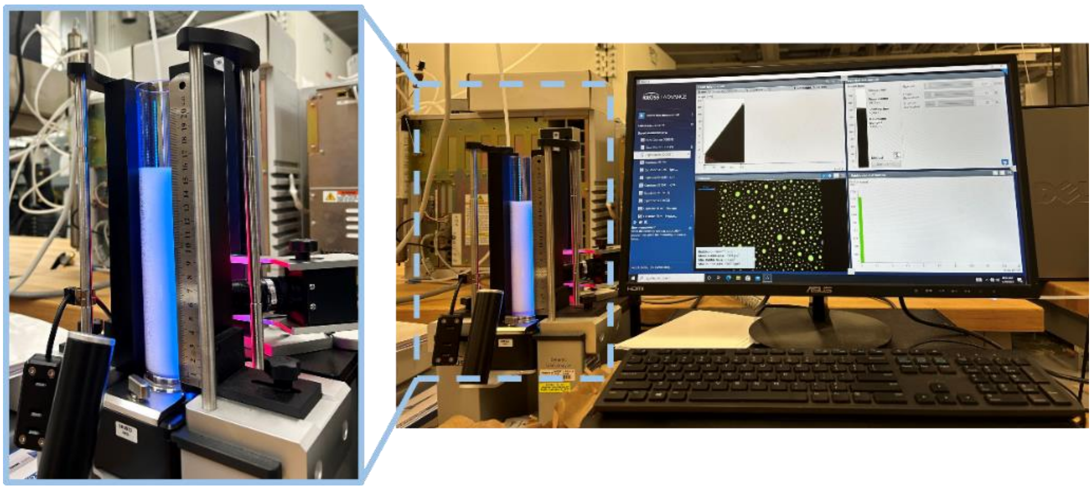

Figure 2. A photo of the dynamic foam analyzer (DFA) setup.

Once the foam was generated, the surfactant solution was swiftly injected at the foam's base using a 25 mL syringe fitted with a 250 mm needle. The injection was completed within 25 s to elevate the interface height, enabling the capture of foam images at the interface. On the other hand, foam/fuel interface experiments were performed according to similar guidelines with a foam/aqueous solution interface. The foam was generated in the cylinder using the previously described method for the foam/fuel interface experiments. Fuel was injected into the bottom of the foam using a 25 mL syringe equipped with a 250 mm needle, completing the injection within 25 s to minimize the effect of foam drainage during fuel interaction. All foam bubble diameters were calculated from images capturing bubbles at the interface and extending up to 4 mm away from it. The study was conducted over a period of 0 to 5000 s to assess the foam's fuel resistance.

3.3. Ignition Experiments and Fuel Transport Quantification

The main components of the ignition test setup include a test container with a diameter of 63 mm and height of 40 mm, a gas cylinder filled with propane, suitable tubing, and a high-speed camera. The ignition times of different fuel types (n-octane, iso-octane, n-heptane, methylcyclohexane, and methylcyclopentane, 25% TMB + 75% n-heptane) and surfactants (Capstone, Glucopon, Capstone+DGBE, Glucopon+DGBE, Capstone+Glucopon, Capstone+Glucopon+DGBE, AFFF) were obtained by pouring approximately 50 mL (height of ~15 mm) of foam generated by the DFA and then injection of 25 mL fuel into the bottom of the foam using a syringe with a blunt tip dispensing 30 mm needle. The fuel injection was completed within 25 s. Then the flame igniter was held ~5 mm above the foam until ignition detection on the surface and the time was recorded for each surfactant/fuel combination. The total ignition tests include five steps, and the real images of each step are presented in Figure 3. Furthermore, the test container was positioned on a scale and zeroed before pouring the foam, allowing for accurate measurement of the foam mass and determination of the expansion ratio for the foams generated by the DFA. All experiments were performed at room temperature. The experiments were repeated at least three times for each fuel and foam case to ensure repeatability and reliability of the experiments.

S1- Empty test container **S2- Pouring foam generated by DFA** **S3- Fuel injection**

S4- Placing the flame $(t_{IT,s})$ **S5- Ignition detection** $(t_{IT,e})$

Figure 3. The steps of the ignition experiments.

3.4. Fuel Transport in Two-Phase Layer Experiments

A two-phase layer experiment was conducted to evaluate the fuel transport into a surfactant solution at a concentration of 5X CMC. The experiment involved layering a fuel mixture of 25% 1,2,4-trimethylbenzene (TMB) and 75% n-heptane over the surfactant solution. This fuel mixture was selected for its practicality and relevance to real-world applications, such as its similarity to gasoline compositions, and to address detection and ignition constraints. N-heptane lacks a detectable signal in the UV-Vis spectrometer due to its low concentration in the surfactant solution, while the fuel mixture provides a strong absorbance peak at 265 nm [44].

The fuel concentration in the bulk solution was measured using a Hitachi U4100 UV-VIS-NIR spectrophotometer (Hitachi High-Technologies Corporation, Tokyo, Japan). The setup, depicted in Figure 4, consisted of a 20 mL glass vial containing a 5 mL syringe for sampling, a 6 × 10 mm cylindrical magnetic stir bar, and 10 mL of surfactant solution, with 5 mL of fuel carefully layered on top. The vial was sealed with parafilm to prevent leakage during the experiments.

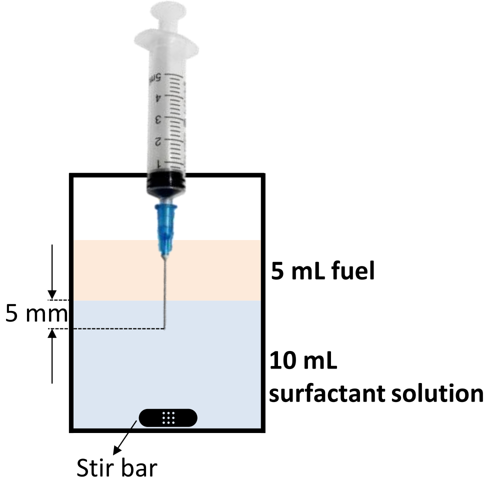

Figure 4. Schematic of the two-phase layer experimental setup.

Absorbance spectra were recorded after 30 min of mixing at a stirring rate of 50 rpm at room temperature (25 °C). Stirring was stopped immediately before sampling to ensure homogeneity and prevent emulsion formation at the interface. For each measurement, 2 mL of surfactant solution was sampled from 5 mm below the interface (Figure 4), with the syringe needle cleaned between extractions to prevent contamination. The UV-Vis absorption peak in the range of 230–300 nm was monitored, focusing on changes at 265 nm, where absorbance change (%) was used as an indicator of fuel concentration in the solution. The absorbance values with fuel were reported as a percentage change relative to the baseline, which was established using surfactant solutions at 5X CMC on both the reference and sample sides of the spectrophotometer. Higher absorbance change values corresponded to greater fuel transport into the surfactant solution.

Each two-phase experiment was repeated at least three times to ensure reliability and reproducibility.

4. Results

This section presents the quantification of fuel transport through foams prepared using surfactant solutions, highlighting the effects of surfactant mixtures and DGBE. Results include measurements of fuel transport through foam layers and analyses of the aqueous solution/foam and fuel/foam interfaces. Additionally, data on fuel transport through bulk surfactant solutions are provided.

4.1. Quantification of Fuel Transport Through Generated Foams

The ignition time for foam prepared using each surfactant is presented in Figure 5. A larger ignition time corresponds to a higher fuel resistance. The minimum ignition times were obtained with single surfactants without any additive (Capstone and Glucopon).

Among the fuels, methylcyclopentane (MCP) showed the lowest ignition time, around 1020 s with single surfactants. The highest ignition times were observed with n-octane, approximately 4230 s. The fluorinated surfactant (Capstone) and hydrocarbon surfactant (Glucopon) alone had similar ignition times. Adding DGBE to the individual surfactants increased ignition times by a factor of 1.2 to 3.7 compared to formulations without DGBE, thereby enhancing fuel resistance. The Capstone+Glucopon mixture exhibited ignition times that were 2.4 to 5.5 times longer than those of the individual surfactants, demonstrating a synergistic effect of combining fluorocarbon and hydrocarbon surfactants. Adding DGBE to the mixture further increased ignition times by a factor of 3 to 7.3 compared to the individual surfactants, producing the highest ignition times observed in the study. The

Capstone+Glucopon+DGBE formulation and the commercial AFFF demonstrated superior performance over all other surfactant systems, including individual surfactants and their DGBE-enhanced formulations.

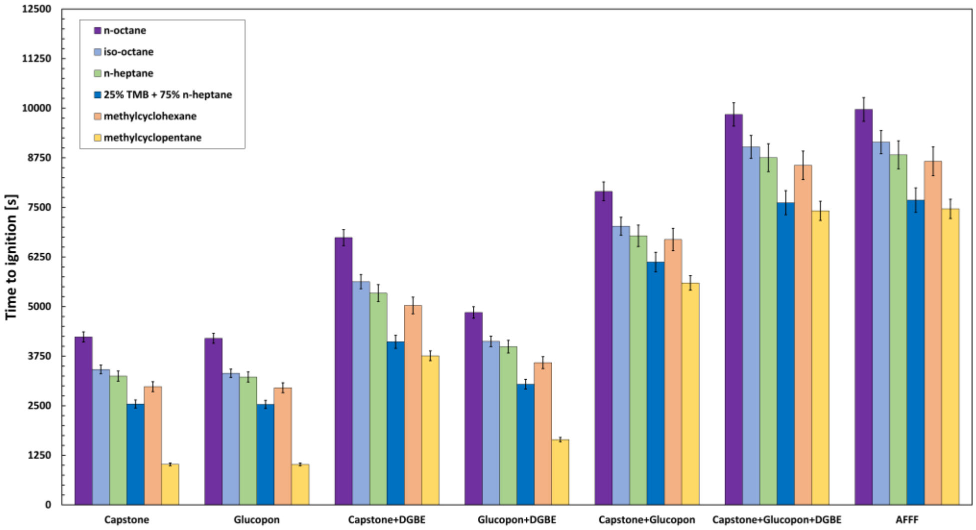

Figure 5. Ignition times for foam prepared using surfactant solutions with each fuel studied.

All trends of ignition times were similar for each surfactant with different fuels. Moderate ignition times were observed with n-heptane, which were higher than those with MCP but lower than with n-octane. The fuel mixture (25% TMB + 75% n-heptane) resulted in much lower ignition times for all surfactants compared to the pure n-heptane. The addition of the DGBE additive to both single surfactants (Capstone and Glucopon) and their mixture resulted in higher ignition times compared to surfactants without the additive.

For all formulations, including fluorine-free surfactants, foam persisted on the fuel surface throughout the entire experiment. This demonstrates that the foam retained its integrity and stability under prolonged exposure to fuels, even those with high vapor pressure and water solubility, such as methylcyclopentane.

4.2. Additive and Fuel Effects on the Generated Foams

4.2.1. Individual Surfactants

The details on the initial foam ($h_{foam\ initial}$) heights and final foam ($h_{foam\ final}$) heights, expansion ratios (ERs), and liquid drainages have been presented for individual surfactants and their mixture with DGBE in Table 3. The mean bubble diameter, foam, and liquid volume with and without fuel are also presented in Figure 6. The foam images were captured when minimal fluctuations in the foam structure were noticed. The foam quality in solutions containing only individual surfactants (without DGBE) is characterized by distinctly larger bubble sizes. In contrast, solutions containing both Capstone and DGBE, as well as Glucopon and DGBE, exhibit noticeably different foam characteristics. It indicates that Capstone has more foamability than Glucopon, providing a higher expansion ratio.

The mean bubble diameter and liquid volume results are presented for Capstone and Glucopon in Figure 6. It can be seen in Figure 6a that Capstone has much larger foam bubbles compared to the Capstone+DGBE foam. On the other hand, Capstone has a higher liquid volume compared to Capstone+DGBE after foam generation. Additionally, adding the fuel shows much larger foam bubbles at the interface. However, this increment is much more pronounced using MCP compared to the n-octane. Additionally, this observation can be supported by the actual foam images of Capstone at the interface with and without DGBE and with and without fuel (MCP and n-octane) which are presented in Figure 7.

Glucopon also shows similar behavior with and without DGBE, providing a decrement in bubble sizes and expansion ratio using DGBE but an increment in 25% liquid drainage time (Table 3). Larger bubbles can be detected with the fuel conditions at the interface; however, much larger bubbles can be detected at the Glucopon-MCP interface. Smaller bubbles can be detected at the interface without fuel conditions (Figure 8). Additionally, adding DGBE decreases the foam bubble size for both foams (Capstone and Glucopon), indicating more stable foams providing an increment in 25% liquid drainage time.

Table 3. Initial ($h_{foam\ initial}$), and final ($h_{foam\ final}$ at 5000 s) foam heights, expansion ratios (ERs), and 25% liquid drainages [s] of Capstone and Glucopon with and without DGBE.

Surfactant	$h_{foam\ initial}$ [mm]	$h_{foam\ final}$ [mm]	Expansion Ratio	25% Liquid Drainage [s]
Capstone	159.9 ± 0.06	102.3 ± 0.30	7.4 ± 0.30	54.1 ± 2.0
Capstone+DGBE	141.4 ± 0.27	106.4 ± 0.29	5.9 ± 0.05	89.5 ± 2.5
Glucopon	137.2 ± 0.32	85.6 ± 0.31	6.0 ± 0.07	50.5 ± 1.8
Glucopon+DGBE	134.8 ± 0.28	98.3 ± 0.34	5.7 ± 0.20	76.8 ± 2.0

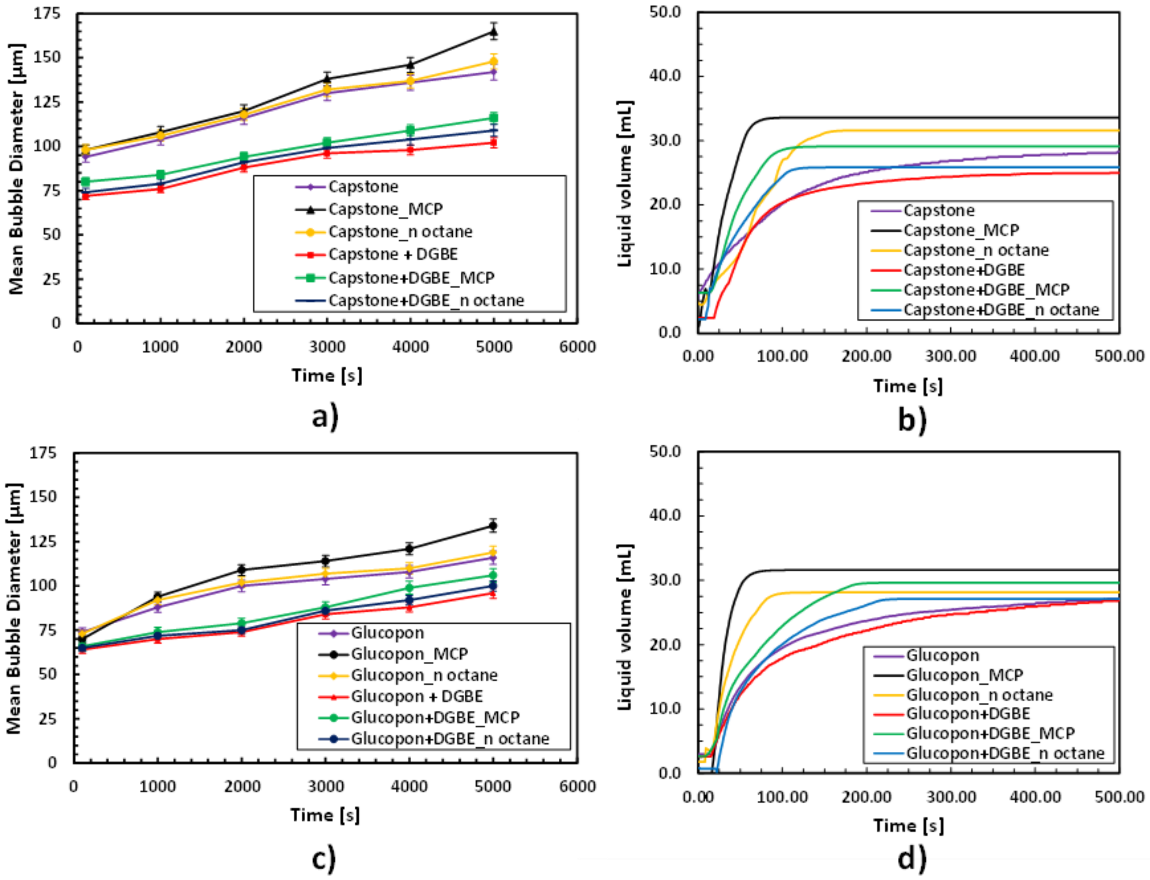

Figure 6. Mean bubble diameter [µm] for (**a**) Capstone and Capstone+DGBE and (**c**) Glucopon and Glucopon+DGBE, liquid volume [mL] over time for (**b**) Capstone and Capstone+DGBE, and (**d**) Glucopon and Glucopon+DGBE.

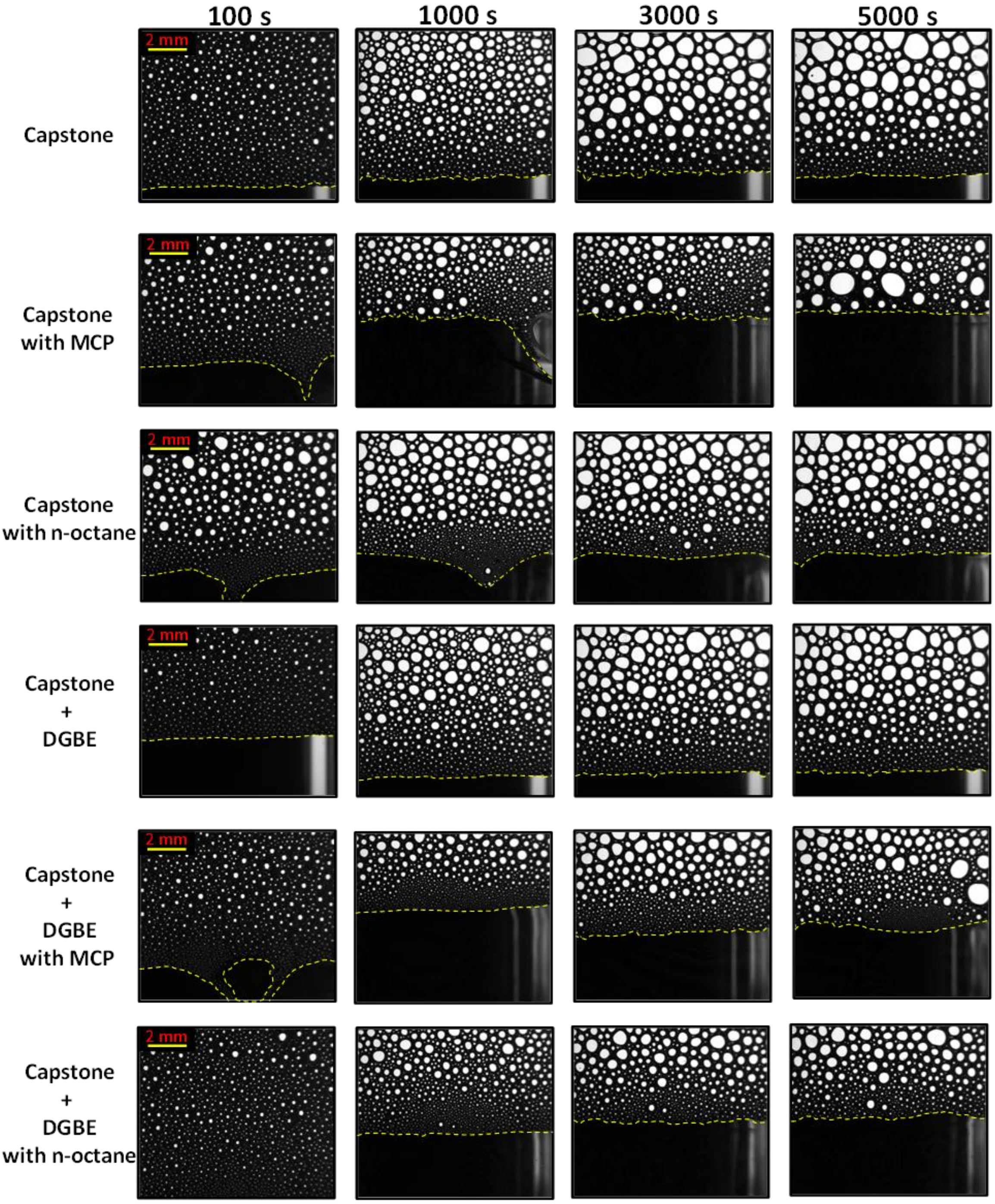

Figure 7. Foam bubble images of the Capstone and Capstone+DGBE with aqueous solution, MCP, and n-octane at the interface. Dashed yellow lines indicate the foam/aqueous solution or foam/fuel interface.

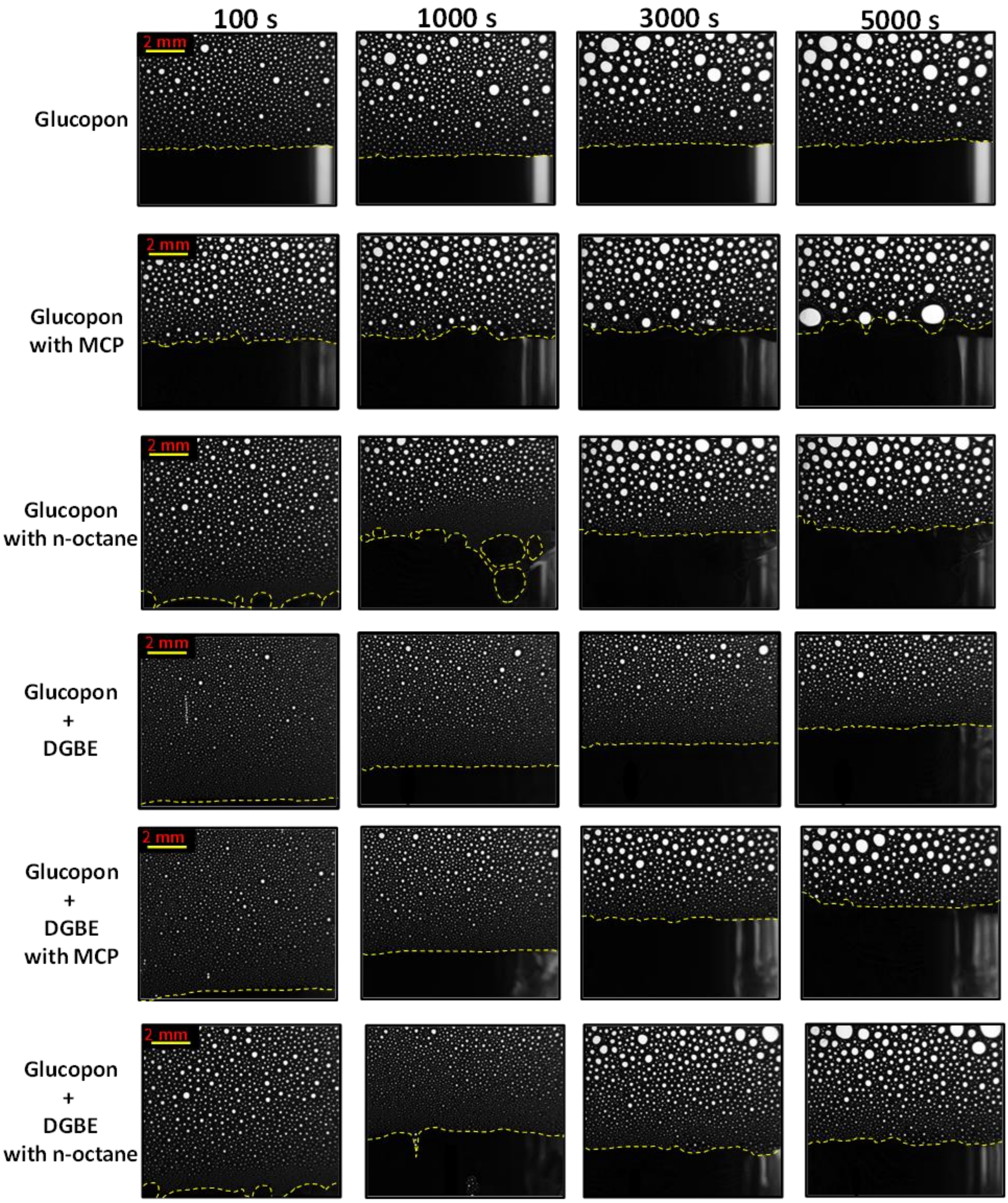

Figure 8. Foam bubble images of the Glucopon and Glucopon+DGBE with aqueous solution, MCP, and n-octane at the interface. Dashed yellow lines indicate the foam/aqueous solution or foam/fuel interface.

It can be seen in Figure 6 that Capstone has a relatively higher mean bubble diameter (larger bubbles) compared to the Glucopon. Among the foams, the coarsening effect was most pronounced in Capstone foam, resulting in larger bubble sizes at t = 5000 s compared to Glucopon (Figure 6). On the other hand, Glucopon foam exhibited the least significant coarsening effect, with relatively smaller bubble sizes at the same time point (5000 s).

4.2.2. Surfactant Mixtures

The effect of DGBE on foams is revealed using the mixture of the individual surfactants with the presence and absence of DGBE. The initial foam ($h_{foam\ initial}$) heights and final foam ($h_{foam\ final}$) heights, expansion ratios (ERs), and 25% liquid drainage times are given for Capstone+Glucopon, Capstone+Glucopon+DGBE, and AFFF in Table 4. The results show that the DGBE affects mean bubble diameter, and it might increase the foam stability after a time ($t \geq 1000$ s). Even though the DGBE effect is more pronounced for individual surfactants (only Capstone and Glucopon), the mixture of the surfactants (Capstone+Glucopon) is also remarkably affected by additive (DGBE) in terms of liquid drainage and mean bubble diameter. The foam quality can be described as having a distinctly larger bubble size and increased translucency in the solution containing only Capstone+Glucopon. In contrast, the solution containing both Capstone, Glucopon, and additive (DGBE) exhibits more stable foam providing smaller foam bubbles and a higher 25% liquid drainage time.

Table 4. Initial ($h_{foam\ initial}$), and final foam ($h_{foam\ final}$ at 5000 s) heights, expansion ratios (ERs), and 25% liquid drainages [s] of a mixture of individual surfactants (Capstone+Glucopon), Capstone+Glucopon+DGBE, and AFFF.

Surfactant	$h_{foam\ initial}$	$h_{foam\ final}$	**Expansion Ratio**	**25% Liquid Drainage [s]**
Capstone+Glucopon	156.3 ± 0.16	135.9 ± 0.18	5.9 ± 0.10	70.0 ± 1.0
Capstone+Glucopon+DGBE	154.2 ± 0.27	145.4 ± 0.22	5.8 ± 0.20	181.1 ± 4.0
AFFF	162.3 ± 0.12	154.6 ± 0.23	6.1 ± 0.50	178.4 ± 1.0

The mixture foam (Capstone+Glucopon) drained more significantly than that with DGBE (Capstone+Glucopon+DGBE). The addition of the DGBE additive provides more gradual increases in the liquid volume. Moreover, the liquid within the foam starts to drain after the foam is generated, leading to the coarsening of bubbles and an increase in the mean bubble diameters. This is more pronounced in the surfactant mixture without DGBE (Capstone+Glucopon) compared to the case with DGBE (Captone+Glucopon+DGBE). From $t \approx 2000$ s onwards, the appearance of stable small bubbles at the corners of larger bubbles was observed, consistent with previous observations [13,45].

The mixture of Capstone and Glucopon produced foam with distinct characteristics, showing larger bubble sizes and a more translucent appearance. On the other hand, Capstone+Glucopon+DGBE, containing the additive (DGBE), exhibited a different foam quality, displaying reduced bubble size and improved foam stability. The mean bubble diameter and liquid volume with respect to time are presented in Figure 9. The results have shown that Capstone+Glucopon+DGBE and commercial AFFF have shown similar foam behavior by providing almost the same mean bubble diameter up to 1000 s. After that point (1000 s), the increment in mean bubble diameter and so higher liquid volume were detected in both foams. These results show that surfactant mixtures with DGBE and commercial AFFF have similar foam behavior.

The foam images of Capstone+Glucopon and Capstone+Glucopon+DGBE at the interface are presented in Figure 10. The results demonstrate that MCP consistently leads to higher liquid drainage for all surfactant mixtures, Capstone+Glucopon, Capstone+Glucopon+DGBE, and AFFF, compared to n-octane. The addition of DGBE additive reduces the amount of liquid drainage for both fuels, although a higher volume of drained surfactant is still observed in the absence of DGBE. Regarding bubble size, the largest mean bubble diameter is observed with MCP for Capstone+Glucopon, indicating that MCP produces larger, less stable bubbles in this mixture. In contrast, the addition of DGBE results in smaller mean bubble diameters for Capstone+Glucopon+DGBE and AFFF, with AFFF showing slightly larger but still similar bubble sizes compared to Capstone+Glucopon+DGBE.

The dynamic behavior of bubbles at the interface, initially smaller, then larger, highlights the foam's evolving stability over time. The pronounced effect of DGBE is evident in the more controlled and stable bubble formation, which contributes to improved foam performance and fuel resistance. Overall, the inclusion of DGBE significantly enhances the foam's stability and fuel resistance, making it a crucial additive for optimizing foam properties.

Figure 10 shows foam bubble images at the interface with the aqueous surfactant solution, MCP, and n-octane for Capstone+Glucopon and Capstone+Glucopon+DGBE mixtures. Similarly, Figure 11 presents images under the same conditions for the Capstone+Glucopon+DGBE mixture and AFFF. The images reveal distinct differences in bubble size and stability depending on the fuel used. Without fuel conditions, all surfactant mixtures show smaller bubbles at the interface, indicating more stable foam structures under these conditions. In contrast, with MCP (Figures 10 and 11), larger bubbles are observed, suggesting that MCP leads to less stable foam compared to n-octane by providing more coarsening at the interface (Figure 9).

Among the surfactant mixtures, Capstone+Glucopon produces the largest bubbles with MCP, while Capstone+Glucopon+DGBE and AFFF exhibit smaller bubbles. This trend highlights that the addition of DGBE or the use of AFFF results in more controlled bubble sizes compared to Capstone+Glucopon alone. Notably, the bubble sizes for AFFF and Capstone+Glucopon+DGBE are similar, indicating that both formulations achieve comparable foam stability and bubble size distribution with MCP. These observations underline the significant role of fuel type and additives in influencing foam bubble characteristics. The smaller bubbles with n-octane suggest a more stable foam structure, whereas the larger bubbles with MCP and the comparative results with different surfactant mixtures highlight the effectiveness of DGBE in enhancing foam stability and reducing bubble size.

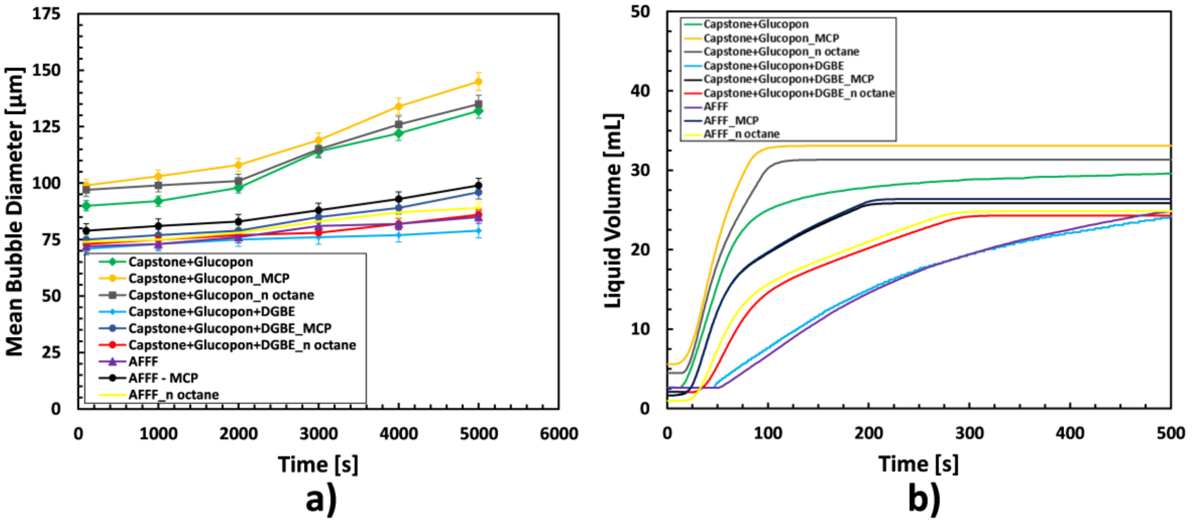

Figure 9. Effect of fuel on mixed surfactant foams: (**a**) foam bubble diameters for Capstone+Glucopon, Capstone+Glucopon+DGBE, and AFFF with and without fuel (MCP and n-octane), (**b**) liquid volume for Capstone+Glucopon, Capstone+Glucopon+DGBE, and AFFF with and without MCP and n-octane.

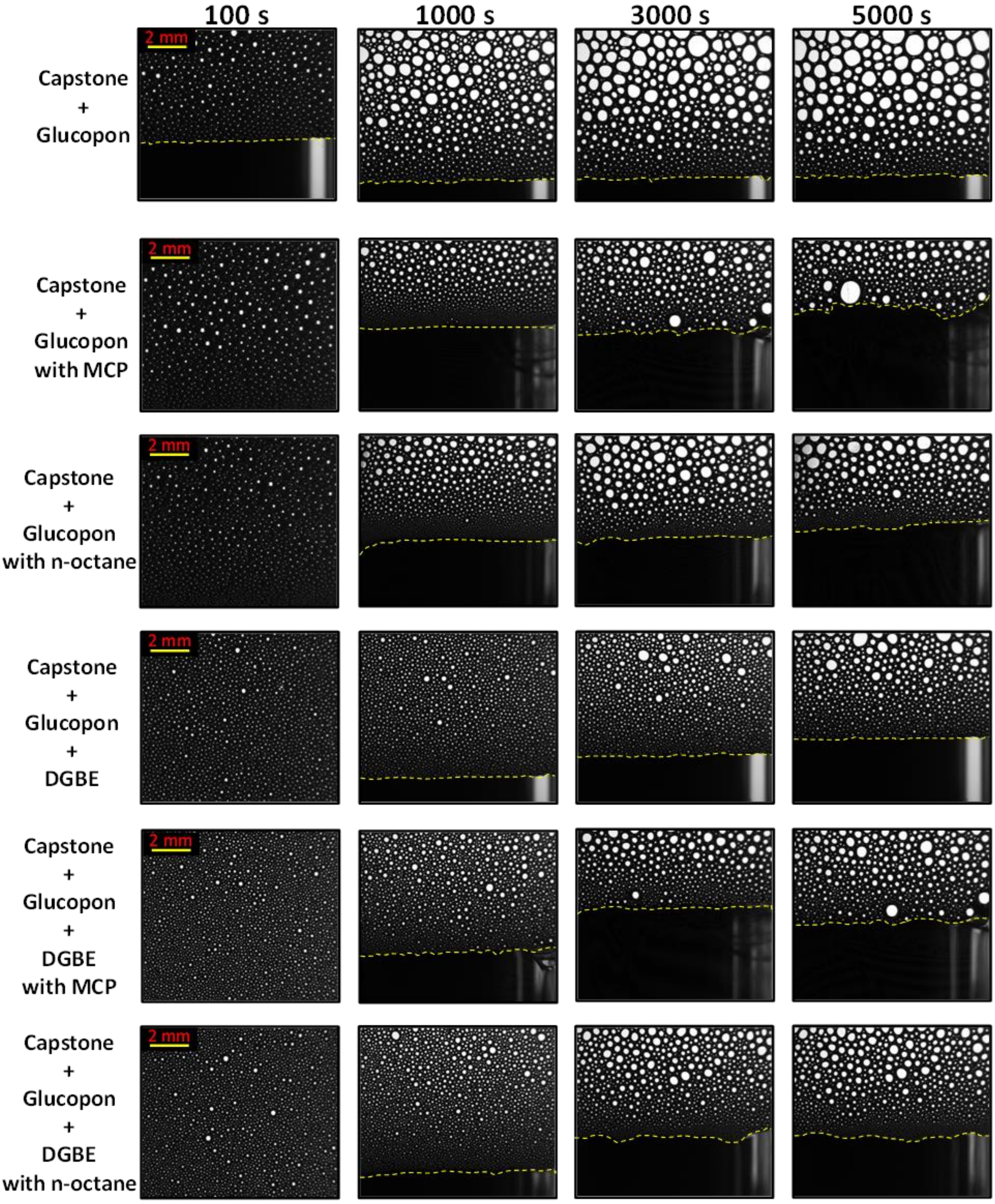

Figure 10. Foam bubble images of the mixture of Capstone+Glucopon and Capstone+Glucopon+DGBE with the aqueous solution, MCP, and n-octane at the interface. Dashed yellow lines show the foam/aqueous solution or foam/fuel interface.

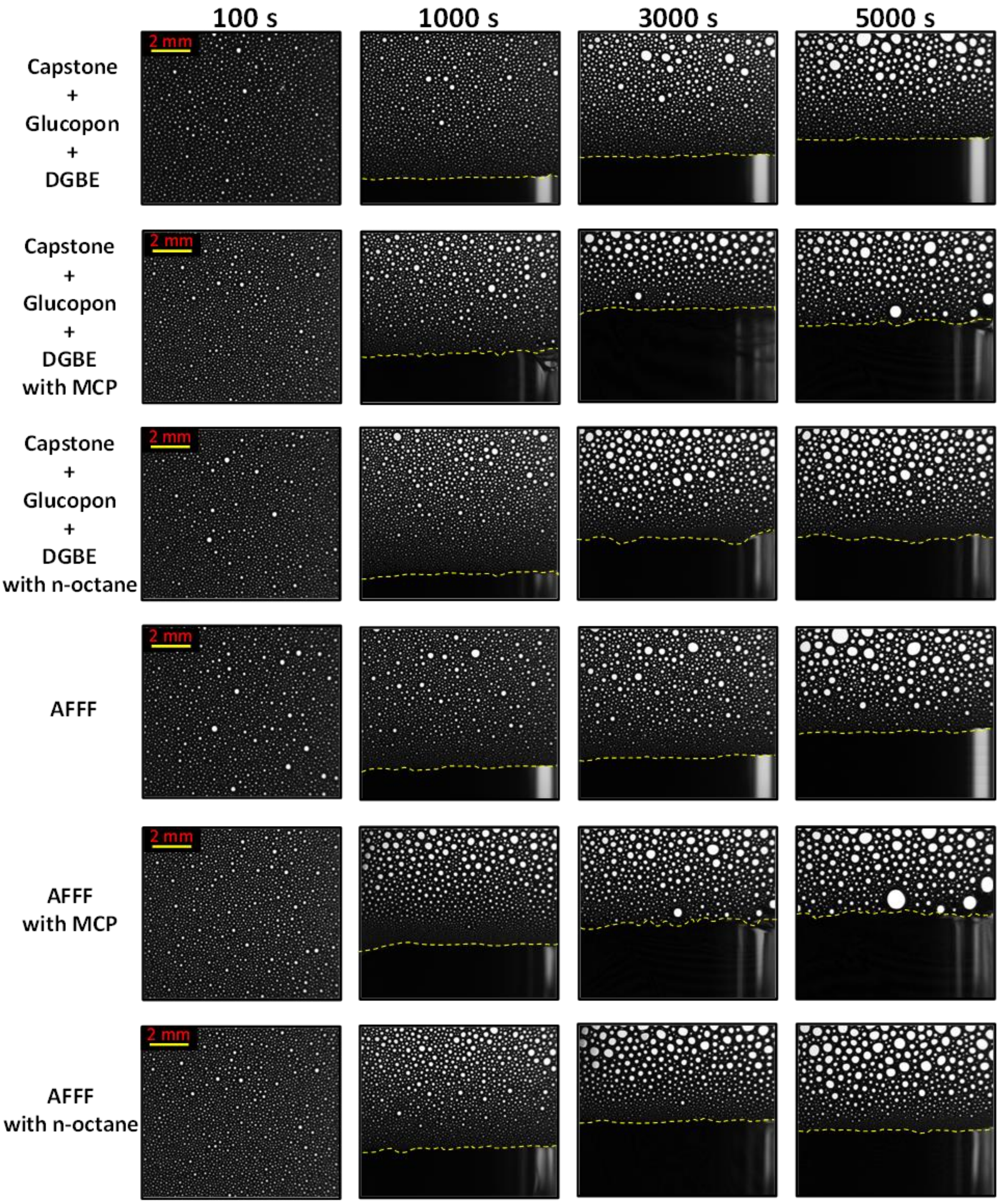

Figure 11. Foam bubble images of the mixture of Capstone+Glucopon+DGBE and AFFF with the aqueous solution, MCP, and n-octane at the interface. Dashed yellow lines show the foam/aqueous solution or foam/fuel interface.

4.3. Fuel Transport Through Aqueous Solution

The absorbance change (%) results from the UV-Vis spectra using a fuel mixture (25% TMB + 75% n-heptane) are shown in Figure 12a,b, where higher absorbance values indicate higher fuel concentrations in the aqueous surfactant solutions. The use of percentage change in absorbance relative to the baseline measurements allowed normalization of the data and accounting for variations in the baseline absorbance of different surfactant solutions. By expressing the changes as a percentage, the results became more directly comparable across different surfactant formulations, ensuring consistency despite variations in initial baseline values.

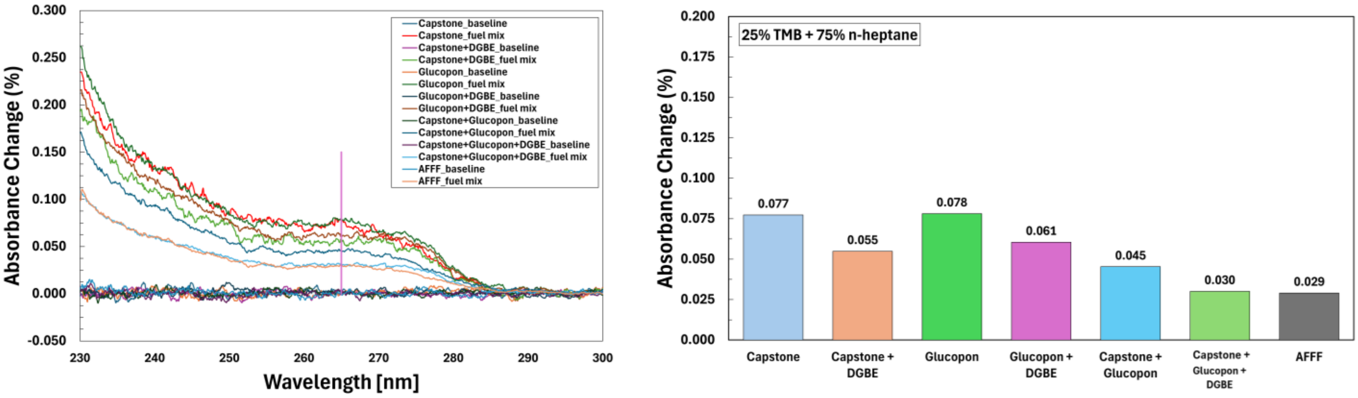

a) **b)**

Figure 12. Absorbance Change (%) of surfactant solutions with fuel mixture: (**a**) UV-Vis spectra in the 230–300 nm range, and (**b**) absorbance change (%) at 265 nm.

Capstone and Glucopon exhibited similar absorbance values of 0.077 and 0.078, respectively, with the fuel mixture. The addition of DGBE to the single surfactants (Capstone+DGBE and Glucopon+DGBE) resulted in lower fuel concentrations compared to their counterparts without DGBE. The mixture of single surfactants (Capstone+Glucopon) further reduced the fuel transported into the aqueous solution. The highest fuel resistance was observed with the addition of DGBE to the surfactant mixture (Capstone+Glucopon+DGBE), which showed the lowest absorbance values, indicating minimal fuel transport. Notably, Capstone+Glucopon+DGBE and commercial AFFF exhibited similar absorbance values, demonstrating comparable fuel resistance.

5. Discussion

Results from this study demonstrate that fuel type, foam bubble distribution, and surfactant solution mixture all significantly influence the fuel transport through the foam. The fuels selected, n-octane, iso-octane, n-heptane, methylcyclohexane, methylcyclopentane (MCP), and a mixture of 25% trimethylbenzene with 75% n-heptane, were chosen to represent a range of vapor pressures, water solubilities, and molecular structures. Among these, n-octane and MCP were selected for detailed analysis of the foam–fuel interface behavior because they represent the extremes in ignition times: n-octane exhibited the longest ignition times, indicating the lowest fuel transport, while MCP showed the shortest ignition times, indicating the fastest fuel transport. An additional explanation is provided below on how these parameters may be affecting fuel transport.

Shorter ignition times (i.e., faster fuel transport through the foam) were observed for fuels with higher vapor pressure and water solubility (see Figure 5 and Table 1). In cases where fuels with different vapor pressures but similar water solubilities (n-octane versus iso-octane, methylcyclohexane versus methylcyclopentane), the fuel with higher vapor pressure (iso-octane, methylcyclopentane) exhibited shorter ignition times, indicating faster fuel transport compared to the fuel with lower vapor pressure [28]. The higher vapor pressure will allow more fuel to be stored in bubbles, thus increasing the fuel concentration differences between adjacent bubbles. These higher gradients in fuel concentrations are believed to help transport the fuel more readily through the foam compared with fuels that have lower vapor pressure.

Increasing the water solubility of the fuel also resulted in shorter ignition times (see Figure 5 and Table 1). In comparing fuels with similar vapor pressures but different water solubilities (iso-octane, heptane, methylcyclohexane), increasing the water solubility resulted in shorter ignition times. Increasing the water solubility allows for more fuel to be transported into the aqueous part of the foam at the fuel–foam interface and the lamella between bubbles. Once in the liquid lamella, the surfactant micelles are able to assist in transporting the fuels to an adjacent bubble, accelerating the transport through the foam. Fuels with lower water solubility require the surfactant to attach to the fuel primarily at the interface, which limits the amount of fuel transport. Adding a polar fuel to a non-polar fuel has a similar effect. The fuel mixture of 25% TMB and 75% n-heptane demonstrates enhanced fuel solubility compared with only heptane, resulting in shorter ignition times due to increased fuel transport through the foam. This is in part why gasoline is more difficult to extinguish compared with heptane in qualification testing [26].

The higher solubility and higher vapor pressure of MCP fuel were observed to cause more rapid Ostwald ripening of the bubbles at the interface, indicating more rapid fuel transport into the foam. As seen in Figures 8–12 there are initially smaller bubbles at the fuel–foam interface in all cases. In cases with no fuel and n-octane, this layer of small bubbles is maintained at the interface, allowing more solution to be maintained at the interface and indicating less transport into the smaller bubbles. With the higher vapor pressure and higher solubility of MCP fuel, these bubbles at the interface and above are observed to grow more with time, indicating fuel transport into the foam. This coarsening also makes the lamella between bubbles become thinner to reduce the fuel transport path length across the solution between bubbles, which may also enhance fuel transport [13].

The surfactant solution mixtures or adding DGBE to the surfactant solutions improves foam stability (see Tables 3 and 4) by slowing down Ostwald ripening. The foam height data further illustrate this improvement: individual surfactants (Capstone and Glucopon) experienced substantial foam height reductions of approximately 36% and 38%, respectively, after 5000 s, indicating lower foam stability. In contrast, the Capstone+Glucopon mixture exhibited a much smaller reduction of 13%, highlighting the synergistic effect of combining fluorocarbon and hydrocarbon surfactants. The addition of DGBE to the mixture (Capstone+Glucopon+DGBE) further enhanced foam stability, resulting in a minimal foam height reduction of 6%. Notably, the Captone+Glucopon+DGBE and AFFF formulations exhibited the least foam decay (6% and 5%, respectively), confirming their superior stability under similar conditions. The smaller bubbles formed in the presence of DGBE present are more resistant to disproportionation, meaning that gas transfer from smaller to larger bubbles is reduced. This effect prolongs the life of the foam, maintaining a dense barrier and effectively slowing down fuel transport through the foam structure. By resisting bubble growth and coalescence, DGBE-enhanced foams demonstrate increased resistance to fuel penetration, higher retention of liquid in the foam matrix, and overall improved fire suppression performance. As a result, the foam exhibited enhanced stability with the surfactant solution mixtures and adding DGBE, as foams with smaller bubbles tend to drain more slowly [13] and resist disproportionation through Ostwald ripening [46].

Faster liquid drainage is observed initially in the presence of fuel. Figure 13 shows the interface of Glucopon foam with aqueous surfactant solution and both fuels, MCP and n-octane, at 100 s and 1000 s. Foam drainage was more pronounced with MCP, especially within the first 300 s (see Figure 6), suggesting a strong initial interaction that leads to rapid liquid loss. This early drainage promotes faster fuel transport through the foam, contributing to shorter ignition times with MCP. In contrast, foams exposed to n-octane showed less initial drainage, indicating a slower interaction and greater stability over time compared to MCP fuel. Without fuel, the foam drains gradually and maintains a stable structure due solely to the surfactant solution (Figure 6), with more stable, smaller bubbles.

The presence of fuel disrupts foam stability by thinning or breaking the surfactant film, resulting in faster drainage and larger, less stable bubbles (see Figures 6 and 9).

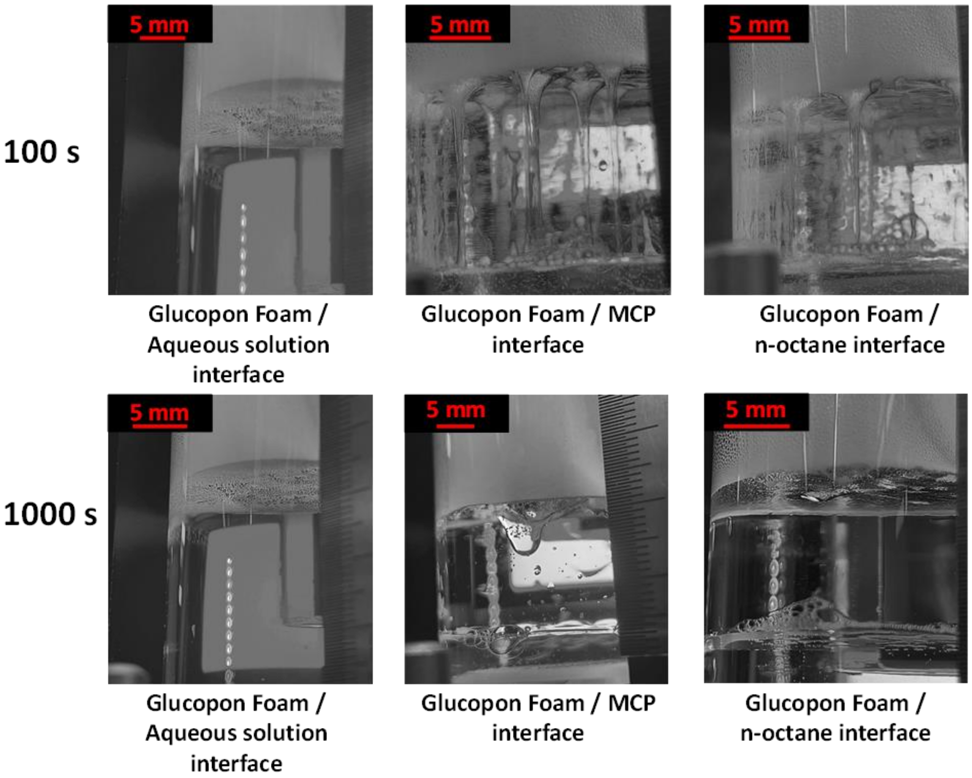

Figure 13. Glucopon foam interfaces with aqueous surfactant solutions and fuels (MCP and n-octane) at 100 s and 1000 s.

The ignition time and two-phase layer results demonstrate that surfactant solution mixtures and DGBE additives influence fuel transport. Capstone and Glucopon alone display similar ignition times, suggesting comparable fuel resistance, likely due to similar fuel uptake in the surfactant bulk (Figure 12). Adding DGBE enhances fuel resistance in both cases, with significantly less fuel in the aqueous surfactant solution compared to single surfactants, but Capstone+DGBE shows notably lower fuel transport than Glucopon+DGBE. This suggests that DGBE has a more pronounced stabilizing effect on Capstone, likely due to its unique fluorocarbon properties, resulting in longer ignition times and greater resistance to fuel penetration. Additionally, the mixture of Capstone and Glucopon shows higher fuel resistance than the individual surfactants or their DGBE-containing versions (Capstone+DGBE and Glucopon+DGBE), suggesting a synergistic improvement in foam stability and fuel blocking (less fuel concentration in the aqueous surfactant solution).

The combination of Capstone, Glucopon, and DGBE produced the longest ignition times, underscoring the surfactant mixture's role in enhancing fuel resistance and foam stability with smaller, more stable bubbles, and low fuel transport through the bulk, which is advantageous for fire suppression. These results align with prior studies [33] that demonstrated improved performance of fluorocarbon-based surfactants with DGBE. Notably, the fuel transport resistance and stability of the Capstone+Glucopon+DGBE system resemble those of commercial AFFF, suggesting both systems provide comparable fuel-blocking and fire suppression capabilities enhancing foam stability with smaller, more stable bubbles, indicating superior fuel blocking and faster fire suppression potential [9,11,33]. This study highlights the potential of surfactant solution mixtures and additives like DGBE for optimizing firefighting foams in diverse fire scenarios. The findings on the enhanced ignition times and fuel resistance of Capstone+Glucopon+DGBE formulations align with previous reports of synergistic interactions between fluorocarbon and hydrocarbon surfactants in mixed systems [9].

While this study primarily focused on measuring foam performance metrics such as ignition time, liquid drainage, and interfacial properties, it is important to acknowledge the role of surfactant–fuel compatibility in influencing foam stability and fuel transport. The results indirectly suggest that compatibility plays a role, as observed through variations in fuel transport rates and foam stability with different fuels. For example, fuels with higher solubility, such as methylcyclopentane, exhibited faster transport through the foam, indicating different interactions with the surfactant-stabilized structure. However, to gain a more direct understanding of surfactant–fuel compatibility, future studies could incorporate additional experiments to quantify these effects. This approach would provide a more comprehensive understanding of the interplay between surfactant formulations and fuel properties. The results presented here offer a strong foundation for exploring these interactions further in subsequent work.

6. Conclusions

An experimental study was conducted to explore the impact of fuel type and surfactant solution on fuel transport through a layer of foam. The results indicate that the fuel type, foam structure at the interface, and fuel transport into the surfactant solution play a role in the overall fuel transport through the foam. Each factor contributes differently to fuel resistance, with fuel type affecting drainage rates, bubble size impacting foam stability, and surfactant mixtures like those with DGBE further enhancing fuel-blocking capability. The findings provide significant insights for optimizing firefighting foam formulations in real-world scenarios. The main findings from this study can be summarized as follows:

- Despite differences in bubble sizes at the Capstone and Glucopon interface, both surfactants show similar fuel resistance, as indicated by comparable fuel levels in solution. DGBE notably enhances their performance, increasing ignition times and reducing fuel transport into the bulk solution, thus improving fuel resistance.
- The Capstone+Glucopon mixture shows higher fuel resistance than individual surfactants, enhancing foam stability and reducing fuel transport. Adding DGBE further improves these properties, making the Capstone+Glucopon+DGBE mixture more effective at resisting fuel transport than the mixture without DGBE.
- The DGBE-added mixture (Capstone+Glucopon+DGBE) and commercial AFFF show the least foam decay (6% and 5%, respectively), underscoring their superior stability under similar conditions. The enhanced stability of these formulations, combined with reduced drainage, longer ignition times, and lower fuel concentration in the bulk solution, highlights the critical role of surfactant composition and DGBE in improving fuel resistance for fire suppression.
- Fuels interact differently with surfactant foams: MCP's higher solubility and vapor pressure lead to larger bubbles, increased liquid drainage, and accelerated Ostwald ripening, while n-octane's lower solubility and vapor pressure support smaller, more stable bubbles with less drainage. This highlights the need for surfactant-additive combinations tailored to specific fuel properties to enhance foam stability and fire suppression.
- Fuels with higher vapor pressure and solubilities, like methylcyclopentane and methylcyclohexane, lead to consistently shorter ignition times across all foam formulations, as increased solubility enhances fuel transport through the foam. Mixing fuels, such as 25% TMB with 75% n-heptane, further boosts solubility, resulting in even shorter ignition times.

By directly linking foam performance to fuel properties, this study provides valuable insights for developing new firefighting foam formulations. The findings highlight the importance of understanding the interactions between surfactants, additives, and fuel types to improve foam stability and fuel resistance. While the experiments were conducted under controlled environmental conditions, the results offer a foundation for future research aimed at validating these findings in real-world industrial or field applications, where environmental factors such as temperature, humidity, and wind may further influence foam performance.

Author Contributions: Conceptualization, A.A., B.Y.L.; methodology, A.A., B.Y.L.; software, A.A., B.Y.L.; validation, A.A.; formal analysis, A.A.; investigation, A.A.; data curation, A.A., B.Y.L.; writing—original draft preparation, A.A., B.Y.L.; writing—review and editing, A.A., R.Q., B.Y.L.; visualization, A.A.; supervision, B.Y.L.; project administration, R.Q., B.Y.L.; funding acquisition, B.Y.L. All authors have read and agreed to the published version of the manuscript.

Funding: This research was funded by the U.S. SERDP program through Contract No. W912HQ22C0028.

Institutional Review Board Statement: Not applicable.

Informed Consent Statement: Not applicable.

Data Availability Statement: The original contributions presented in this study are included in the article. Further inquiries can be directed to the corresponding authors.

Acknowledgments: This work was made possible by the use of Virginia Tech's Materials Characterization Facility, which is supported by the Institute for Critical Technology and Applied Science, the Macromolecules Innovation Institute, and the Office of the Vice President for Research and Innovation. The authors thank Rezawana Islam for providing CMC data.

Conflicts of Interest: The authors declare no conflicts of interest.

References

1. Sheng, Y.; Xue, M.; Ma, L.; Zhao, Y.; Wang, Q.; Liu, X. Environmentally Friendly Firefighting Foams Used to Fight Flammable Liquid Fire. *Fire Technol.* **2021**, *57*, 2079–2096. [CrossRef]
2. Osei-Bonsu, K.; Shokri, N.; Grassia, P. Foam stability in the presence and absence of hydrocarbons: From bubble- to bulk-scale. *Colloids Surf. A Physicochem. Eng. Asp.* **2015**, *481*, 514–526. [CrossRef]
3. Hinnant, K.M.; Conroy, M.W.; Ananth, R. Influence of fuel on foam degradation for fluorinated and fluorine-free foams. *Colloids Surf. A Physicochem. Eng. Asp.* **2017**, *522*, 1–17. [CrossRef]
4. Sheng, Y.; Jiang, N.; Lu, S.; Li, C. Fluorinated and fluorine-free firefighting foams spread on heptane surface. *Colloids Surf. A Physicochem. Eng. Asp.* **2018**, *552*, 1–8. [CrossRef]
5. Narsimhan, G. Drainage of particle stabilized foam film. *Colloids Surf. A Physicochem. Eng. Asp.* **2016**, *495*, 20–29. [CrossRef]
6. Yang, L.; Min, R.; Wang, G.; Wu, Q.; Qu, A.; Zhuo, C.; Wang, Q.; Ruan, X. Evaluation of interfacial, micellar, and foaming properties of the solutions comprising fluorocarbon surfactant, cocamidopropyl betaine, and Gleditsia saponin as fire-extinguishing agents. *Chem. Eng. Sci.* **2023**, *272*, 118590. [CrossRef]
7. Li, Q.; Li, S.; Yu, Y.; Yu, X.; Qiu, K.; Xu, M.; Lu, S.; Lin, J. Synergistic enhancement of foam stability by nanocellulose and hydrocarbon surfactants. *Chem. Eng. Sci.* **2024**, *299*, 120418. [CrossRef]
8. Hinnant, K.M.; Giles, S.L.; Ananth, R. Measuring fuel transport through fluorocarbon and fluorine-free firefighting foams. *Fire Saf. J.* **2017**, *91*, 653–661. [CrossRef]
9. Hinnant, K.M.; Giles, S.L.; Snow, A.W.; Farley, J.P.; Fleming, J.W.; Ananth, R. An Analytically Defined Fire-Suppressing Foam Formulation for Evaluation of Fluorosurfactant Replacement. *J. Surfactants Deterg.* **2018**, *21*, 711–722. [CrossRef]
10. Lattimer, B.Y.; Hanauska, C.P.; Scheffey, J.L.; Williams, F.W. The use of small-scale test data to characterize some aspects of fire fighting foam for suppression modeling. *Fire Saf. J.* **2003**, *38*, 117–146. [CrossRef]
11. Ananth, R.; Snow, A.W.; Hinnant, K.M.; Giles, S.L.; Farley, J.P. Synergisms between siloxane-polyoxyethylene and alkyl polyglycoside surfactants in foam stability and pool fire extinction. *Colloids Surf. A Physicochem. Eng. Asp.* **2019**, *579*, 123686. [CrossRef]
12. Hinnant, K.M.; Giles, S.L.; Smith, E.P.; Snow, A.W.; Ananth, R. Characterizing the Role of Fluorocarbon and Hydrocarbon Surfactants in Firefighting-Foam Formulations for Fire-Suppression. *Fire Technol.* **2020**, *56*, 1413–1441. [CrossRef]

13. Kennedy, M.J.; Conroy, M.W.; Dougherty, J.A.; Otto, N.; Williams, B.A.; Fleming, J.W. Bubble coarsening dynamics in fluorinated and non-fluorinated firefighting foams. *Colloids Surf. A Physicochem. Eng. Asp.* **2015**, *470*, 268–279. [CrossRef]
14. Zhou, T.; Liu, Y.; Wu, W.; Zhou, T. Experimental Study and Application of Unmanned Aerial Vehicle Releasing Fire-Extinguishing Bomb on Transmission Line Wildfires. *Fire* **2024**, *7*, 456. [CrossRef]
15. Sheng, Y.; Jiang, N.; Lu, S.; Wang, Q.; Zhao, Y.; Liu, X. Study of Environmental-Friendly Firefighting Foam Based on the Mixture of Hydrocarbon and Silicone Surfactants. *Fire Technol.* **2020**, *56*, 1059–1075. [CrossRef]
16. Sheng, Y.; Peng, Y.; Zhang, S.; Guo, Y.; Ma, L.; Zhang, H. Thermal stability of foams stabilized by fluorocarbon and hydrocarbon surfactants in presence of nanoparticles with different specific surface areas. *J. Mol. Liq.* **2022**, *365*, 29–31. [CrossRef]
17. Yan, L.; Guan, J.; Wang, N.; Wei, Z.; Xu, Z.; Niu, G. Design of fluorine-free foam extinguishing agent with high surface activity, foam stability and pool fire suppression by optimization of surfactant composition and foam system. *Colloids Surf. A Physicochem. Eng. Asp.* **2024**, *693*, 134094. [CrossRef]
18. Qiu, K.; Yu, X.; Li, Q.; Li, H.; Kang, N.; Lu, S. Thermo-responsive fluorine-free foam stabilized by PEO–PPO–PEO triblock copolymer (EO)100(PO)65(EO)100 for pool fire suppression. *SmartMat* **2024**, *5*, 1–14. [CrossRef]
19. Jia, H.; Zeng, J.; Zou, Q.; Zheng, L.; Pan, R. Fluorine-free foaming extinguishing agent: Design route, fire extinguishing performance, foam stability mechanism. *Arab. J. Chem.* **2024**, *17*, 105712. [CrossRef]
20. Hinnant, K.M.; Giles, S.L.; Ananth, R.; Miller, J.H. Exploring synergistic fire suppression of siloxane-glycoside firefighting foam using sulfonated hydrotrope additives to alter surfactant aggregation in solution. *Colloids Surf. A Physicochem. Eng. Asp.* **2022**, *655*, 130219. [CrossRef]
21. Schaefer, T.H.; Dlugogorski, B.Z.; Kennedy, E.M. Sealability properties of fluorine-free fire-fighting foams (FfreeF). *Fire Technol.* **2008**, *44*, 297–309. [CrossRef]
22. Durian, D.J.; Weitz, D.A.; Pine, D.J. Scaling behavior in shaving cream. *Phys. Rev. A* **1991**, *44*, R7902. [CrossRef] [PubMed]
23. Ubal, S.; Lu, J.; Grifoni, R.; Bozzoli, F.; Corvalan, C.M. Coalescence preference in surfactant-laden bubbles of equal size. *Chem. Eng. Sci.* **2022**, *253*, 117550. [CrossRef]
24. Xu, Z.; Guo, X.; Yan, L.; Kang, W. Fire-extinguishing performance and mechanism of aqueous film-forming foam in diesel pool fire. *Case Stud. Therm. Eng.* **2020**, *17*, 100578. [CrossRef]
25. Sheng, Y.; Xue, M.; Zhang, S.; Wang, Y.; Zhai, X.; Ma, L.; Hu, D.; Huang, X. Effect of xanthan gum and silica nanoparticles on improving foam properties of mixed solutions of short-chain fluorocarbon and hydrocarbon surfactants. *Chem. Eng. Sci.* **2021**, *245*, 116952. [CrossRef]
26. Snow, A.W.; Giles, S.; Hinnant, K.; Farley, J.; Ananth, R. Fuel for Firefighting Foam Evaluations: Gasoline vs Heptane. In *NRL Report*; Technical Report No. NRL/MR/6123-19-9865; Naval Research Lab Washington: Washington, DC, USA, 2019.
27. Vicaria, J.M.; Herrera-Márquez, O.; Serrano-Haro, M.; Vidal, A.; Jurado, E.; Jiménez-Pérez, J.L. Optimization of surfactants formulations to stabilise proteases and amylases. *Chem. Eng. Sci.* **2022**, *260*, 117858. [CrossRef]
28. Ateş, A.; Lattimer, B.Y.; Conversano, V. Fuel effects on foams generated using different surfactants. *Fire Saf. J.* **2023**, *141*, 104012. [CrossRef]
29. Yu, X.; Li, F.; Fang, H.; Miao, X.; Wang, J.; Zong, R.; Lu, S. Foaming behavior of fluorocarbon surfactant used in fire-fighting: The importance of viscosity and self-assembly structure. *J. Mol. Liq.* **2021**, *327*, 114811. [CrossRef]
30. Pasc-Banu, A.; Blanzat, M.; Belloni, M.; Perez, E.; Mingotaud, C.; Rico-Lattes, I.; Labrot, T.; Oda, R. Spontaneous vesicles of single-chain sugar-based fluorocarbon surfactants. *J. Fluor. Chem.* **2005**, *126*, 33–38. [CrossRef]
31. Yu, X.; Jiang, N.; Miao, X.; Zong, R.; Sheng, Y.; Li, C.; Lu, S. Formation of stable aqueous foams on the ethanol layer: Synergistic stabilization of fluorosurfactant and polymers. *Colloids Surf. A Physicochem. Eng. Asp.* **2020**, *591*, 124545. [CrossRef]
32. Sheng, Y.; Jiang, N.; Lu, S.; Zhao, Y.; Wang, Q.; Ma, L.; Liu, X. Molecular interaction and foaming property of the mixtures of hydrocarbon, fluorocarbon and silicone surfactants. *J. Mol. Liq.* **2019**, *296*, 111836. [CrossRef]
33. Giles, S.L.; Snow, A.W.; Hinnant, K.M.; Ananth, R. Modulation of fluorocarbon surfactant diffusion with diethylene glycol butyl ether for improved foam characteristics and fire suppression. *Colloids Surf. A Physicochem. Eng. Asp.* **2019**, *579*, 123660. [CrossRef]
34. Xu, Q.; Nakajima, M.; Ichikawa, S.; Nakamura, N.; Roy, P.; Okadome, H.; Shiina, T. Effects of surfactant and electrolyte concentrations on bubble formation and stabilization. *J. Colloid Interface Sci.* **2009**, *332*, 208–214. [CrossRef]
35. Sheng, Y.; Ma, W.; Yu, X.; Ma, L.; Li, Y. Effect of liquid fuel on foamability and foam stability of mixtures of fluorocarbon and hydrocarbon surfactants. *J. Mol. Liq.* **2023**, *388*, 122762. [CrossRef]
36. Kim, D.K.; Ananth, R. Anomalous diffusion of hydrocarbon vapor through an aqueous foam bubble structure. *Colloids Surf. A Physicochem. Eng. Asp.* **2024**, *702*, 134937. [CrossRef]
37. National Center for Biotechnology Information. PubChem Substance Record for SID 134973409, Heptane, Source: ChemIDplus. 2025. Available online: https://pubchem.ncbi.nlm.nih.gov/substance/134973409 (accessed on 21 January 2025).
38. National Center for Biotechnology Information. PubChem Compound Summary for CID 7962, Methylcyclohexane. 2025. Available online: https://pubchem.ncbi.nlm.nih.gov/compound/Methylcyclohexane (accessed on 21 January 2025).

39. National Center for Biotechnology Information. PubChem Compound Summary for CID 7296, Methylcyclopentane. 2025. Available online: https://pubchem.ncbi.nlm.nih.gov/compound/Methylcyclopentane (accessed on 21 January 2025).
40. National Center for Biotechnology Information. PubChem Compound Summary for CID 356, Octane. 2025. Available online: https://pubchem.ncbi.nlm.nih.gov/compound/Octane (accessed on 21 January 2025).
41. National Center for Biotechnology Information. PubChem Compound Summary for CID 7247, 1,2,4-Trimethylbenzene. Available online: https://pubchem.ncbi.nlm.nih.gov/compound/1_2_4-Trimethylbenzene (accessed on 21 January 2025).
42. National Center for Biotechnology Information. PubChem Compound Summary for CID 10907, 2,2,4-Trimethylpentane. 2025. Available online: https://pubchem.ncbi.nlm.nih.gov/compound/2_2_4-Trimethylpentane (accessed on 21 January 2025).
43. Hetzer, R.H.; Kümmerlen, F.; Wirz, K.; Blunk, D. Fire testing a new fluorine-free AFFF based on a novel class of environmentally sound high performance siloxane surfactants. *Fire Saf. Sci.* **2014**, *11*, 1261–1270. [CrossRef]
44. Scherer, M.D.; Oliveira, S.L.; Lima, S.M.; Andrade, L.H.C.; Caires, A.R.L. Determination of the biodiesel content in diesel/biodiesel blends: A method based on fluorescence spectroscopy. *J. Fluoresc.* **2011**, *21*, 1027–1031. [CrossRef] [PubMed]
45. Feitosa, K.; Halt, O.L.; Kamien, R.D.; Durian, D.J. Bubble kinetics in a steady-state column of aqueous foam. *Europhys. Lett.* **2006**, *76*, 683–689. [CrossRef]
46. Dlugogorski, B.Z.; Schaefer, T.H. Compatibility of aqueous film-forming foams (AFFF) with sea water. *Fire Saf. J.* **2021**, *120*, 103288. [CrossRef]

Disclaimer/Publisher's Note: The statements, opinions and data contained in all publications are solely those of the individual author(s) and contributor(s) and not of MDPI and/or the editor(s). MDPI and/or the editor(s) disclaim responsibility for any injury to people or property resulting from any ideas, methods, instructions or products referred to in the content.